JOURNAL OF BACTERIOLOGY, June 1997, p. 3470–3481 Vol. 179, No. 11
0021-9193/97/$04.00+0

Structure and Expression of a Pyrimidine Gene Cluster from the Extreme Thermophile *Thermus* Strain ZO5

MARK VAN DE CASTEELE,[1] PINGGUO CHEN,[1] MARTINE ROOVERS,[1] CHRISTIANE LEGRAIN,[2] AND NICOLAS GLANSDORFF[1,2]*

Department of Microbiology, Vlaams Interuniversitair Instituut voor Biotechnologie and Vrije Universiteit Brussel,[1] and Research Institute of the Ceria-Coovi,[2] B-1070 Brussels, Belgium

Received 28 October 1996/Accepted 20 March 1997

On a 4.7-kbp *Hin*dIII clone of *Thermus* strain ZO5 DNA, complementing an aspartate carbamoyltransferase mutation in *Escherichia coli*, we identified a cluster of four potential open reading frames corresponding to genes *pyrR*, and *pyrB*, an unidentified open reading frame named *bbc*, and gene *pyrC*. The transcription initiation site was mapped at about 115 nucleotides upstream of the *pyrR* translation start codon. The cognate *Thermus pyr* promoter also functions in heterologous expression of *Thermus pyr* genes in *E. coli*. In *Thermus* strain ZO5, *pyrB* and *pyrC* gene expression is repressed three- to fourfold by uracil and increased twofold by arginine. Based on the occurrence of several transcription signals in the *Thermus pyr* promoter region and strong amino acid sequence identities (about 60%) between *Thermus* PyrR and the PyrR attenuation proteins of two *Bacillus* sp., we propose a regulatory mechanism involving transcriptional attenuation to control *pyr* gene expression in *Thermus*. In contrast to *pyr* attenuation in *Bacillus* spp., however, control of the *Thermus pyr* gene cluster would not involve an antiterminator structure but would involve a translating ribosome for preventing formation of the terminator RNA hairpin. The deduced amino acid sequence of *Thermus* strain ZO5 aspartate carbamoyltransferase (ATCase; encoded by *pyrB*) exhibits the highest similarities (about 50% identical amino acids) with ATCases from *Pseudomonas* sp. For *Thermus* strain ZO5 dihydroorotase (DHOase; encoded by *pyrC*), the highest similarity scores (about 40% identity) were obtained with DHOases from *B. caldolyticus* and *Bacillus subtilis*. The enzyme properties of ATCase expressed from truncated versions of the *Thermus pyr* gene cluster in *E. coli* suggest that *Thermus* ATCase is stabilized by DHOase and that the translation product of *bbc* plays a role in feedback inhibition of the ATCase-DHOase complex.

Thermus strain ZO5 is an extremely thermophilic gram-negative carotenoid pigmented bacterium which is closely related to *Thermus aquaticus* YT-1 and to *T. thermophilus* HB8 (10). The optimal growth temperature of *Thermus* strain ZO5 is about 72°C, and the maximum temperature for growth 85°C in rich medium. This microorganism has been studied with respect to antibiotic sensitivity, nutritional pattern, primary metabolism (10), and arginine biosynthesis (57).

The metabolism of pyrimidines in extreme thermophiles deserves investigation from both fundamental and applied points of view. Genes of the pyrimidine biosynthetic pathway have been successfully used as genetic markers in mesophilic procaryotes and lower eucaryotes. Recently, the *pyrE* and *pyrF* genes from *Thermus* sp. were cloned and sequenced in order to provide selectable markers for developing thermophilic cloning vectors (61, 64). The *T. thermophilus* HB8 *pyrH* gene, encoding UMP kinase, was sequenced recently and shown to be located adjacent to the *tsf* gene, which codes for elongation factor Ts (4).

De novo synthesis of pyrimidines involves utilization of energy-rich labile intermediates such as carbamoyl phosphate, phosphoribosyl pyrophosphate (PRPP), and nucleoside triphosphates, raising the question as to how thermodegradation of these compounds is dealt with in thermophilic physiology. Indeed, even members of the hyperthermophilic archaea, growing optimally above 80°C, use the standard de novo route to synthesize UMP (18). It appears that at least one very labile intermediate, carbamoyl phosphate, a common precursor of arginine and pyrimidines, is channeled in the hyperthermophilic archaeon *Pyrococcus furiosus* (27) as well as in *Thermus* strain ZO5 (59).

The conversion of glutamine, bicarbonate, aspartate, and PRPP to UMP is based on six enzyme reactions. In *Thermus*, nothing is known about the first four catalyzed steps of this pathway or about its genetic organization and control of expression. In *Escherichia coli*, the pyrimidine biosynthetic genes are genetically unlinked; the *pyrBI* operon encoding aspartate carbamoyltransferase (ATCase) is regulated through UTP-sensitive transcriptional attenuation (8, 41, 42, 54). In *Bacillus subtilis* and in the extreme thermophile *B. caldolyticus*, all of the *pyr* genes reside in a single operon which also includes two pyrimidine salvage genes: *pyrR*, encoding a uracil phosphoribosyltransferase (UPRTase), and *pyrP*, encoding a uracil permease (15, 16, 39, 55). In *B. subtilis*, a second UPRTase-encoding gene (*upp*) is responsible for most of the UPRTase activity and hence also uracil salvage (31). In *B. subtilis* and probably also in *B. caldolyticus*, expression of the *pyr* operon (gene order *pyrRPBCDAFE*) is regulated by an autogenous transcription attenuation mechanism in which binding of an attenuation protein (*pyrR*) disrupts the formation of the antiterminator secondary structure in three untranslated regions of the transcript (14, 29, 30, 55). In *Pseudomonas aeruginosa* and *P. putida*, the *pyrB* gene, encoding an ATP-inhibited ATCase, overlaps with a so-called *pyrC′* gene, which codes for a dihydroorotase (DHOase)-like protein without activity. Expression of the *pyrC′* gene is required for assembly and function of ATCase. In this case, DHOase activity originates from a *pyrC* gene residing elsewhere on the chromosome (2, 47).

The *pyrB* and *pyrI* genes of *E. coli* code for the catalytic (c) and regulatory (r) chains, respectively, of ATCase. The 320-

* Corresponding author. Mailing address: Department of Microbiology, Onderzoekingsinstituut CERIA-COOVI, 1 Av. E. Gryzon, B-1070 Brussels, Belgium. Phone: 32 2 526 72 75. Fax: 32 2 526 72 73. E-mail: ceriair@ulb.ac.be.

kDa highly cooperative $2c_3:3r_2$ holoenzyme displays ATP activation and is feedback inhibited by UTP and CTP; it has become a model system for the study of regulatory interactions in allosteric proteins (28). The three-dimensional structures for *E. coli* ATCase and the unregulated (c_3) *B. subtilis* ATCase have been described (21, 52). Numerous ATCase sequences are also known (9). Despite these favorable conditions for studying structure-function relationships and molecular mechanisms of enzyme stabilization in thermophilic ATCases, data pertaining to ATCases from thermophiles have remained scarce (16, 38, 58).

In this study, we describe the primary structure and organization of a *Thermus* strain ZO5 gene cluster that contains at least the genes for ATCase and DHOase, two early de novo pyrimidine biosynthetic activities, as well as a gene encoding a salvage enzyme which is also a candidate regulatory protein. Our data indicate that this cluster is expressed in *E. coli* from the *Thermus* strain ZO5 *pyr* promoter and that in *Thermus*, expression of *pyr* genes is regulated by uracil and arginine. Based on the analysis of the nucleotide sequence in the promoter region of the *Thermus pyr* gene cluster, we suggest a mechanism for controlling its expression.

MATERIALS AND METHODS

Growth media and culture conditions. Medium 853 (17) was used as a rich liquid medium and, with 1.5% agar (Difco), as a solid medium for *E. coli*. *E. coli* TG1 and JM101 were used as hosts for recombinant plasmids and for single-stranded phagemid DNA rescue in medium 853 containing 100 μg of ampicillin per ml. *E. coli* starter cultures were in minimal medium 132 (17) containing 0.5% glucose and thiamine (1 μg/ml) in order to select for F′ derivatives. *E. coli* C600 $pyrBI_{1510}$ lacks ACTase, requires proline and uracil, and was used in screening for *pyrB* complementation with recombinant plasmids by testing its growth in minimal medium 132 supplemented with glucose (0.5%), thiamine (1 μg/ml), and proline (100 μg/ml). *E. coli* JM101 was used to monitor expression of the chloramphenicol acetyltransferase (*cat*) gene from vector pKK232-8. This strain was grown in medium 853 containing either ampicillin or chloramphenicol.

Thermus strain ZO5 was grown at 65°C in defined 162 arginine- and uracil-free (AUF) medium (10, 36) with pyruvate (20 mM) and ammonium sulfate (10 mM) as carbon and nitrogen sources, respectively (57). *Thermus* strain ZO5 was also cultured in minimal medium D (7), using the same N and C sources. Pyrimidine gene expression was studied in medium D. To grow *Thermus* strain ZO5 in the presence of excess pyrimidines or arginine, 50 μg of uracil and 100 μg of arginine per ml were used. Pyrimidine starvation of *Thermus* strain ZB1 (see below) was carried out in medium D containing a limiting amount of uracil (4 μg/ml). Solid media for *Thermus* contained 2.5% purified agar (Oxoid).

Isolation of an auxotrophic (*pyrB*) mutant of *Thermus* strain ZO5. One colony of the *Thermus* wild-type strain ZO5 was inoculated in 20 ml of 162 AUF medium containing 50 μg of uracil and 100 μg of the mutagen *N*-methyl-*N*′-nitro-*N*-nitrosoguanidine per ml. Cells were cultured at 65°C to the stationary phase and diluted 400-fold in identical fresh medium for further overnight growth. Without enrichment, the mutagenized population was appropriately diluted in 162 medium and spread on solid 162 AUF medium containing uracil. A total of 1,600 isolated colonies were subsequently screened for the absence of growth on 162 AUF medium. Three uracil auxotrophs were identified, purified, and retested for the Ura^- phenotype. Two Ura^- mutants displayed growth in the presence of orotate. These two mutants (named *Thermus* strains ZB1 and ZB2) lacked ACTase activity. Being characterized by a lower reversion frequency (5×10^{-8} versus 10^{-6}), *Thermus* strain ZB1 was further used in this study.

DNA manipulation and analysis. All enzymes used in the manipulation of DNA were used according to the manufacturer's specifications. Restriction enzymes, T4 DNA ligase, T7 DNA polymerase, alkaline phosphatase, polynucleotide kinase, S1 nuclease, exonuclease III, and Klenow DNA polymerase were purchased from Boehringer Mannheim or Pharmacia. Plasmid preparation, restriction enzyme digests, agarose gel and polyacrylamide gel electrophoresis, DNA ligation, transformation of *E. coli*, and preparation of single-stranded phagemid DNA were carried out as described by Sambrook et al. (44). DNA was sequenced by the method of Sanger et al. (45), using a T7 DNA sequencing kit (Pharmacia). 7-Deaza-dGTP reactions were used to resolve compressions due to the high G+C content of *Thermus* strain ZO5 DNA.

The sequencing strategy for the 4.7-kb *Hin*dIII fragment carrying the *Thermus* strain ZO5 *pyr* gene cluster was as follows. The 2.8-kb *Hin*dIII-*Kpn*I and the 1.9-kb *Kpn*I-*Hin*dIII subfragments of the 4.7-kb *Hin*dIII insert of pTA3 were cloned in two orientations into pBluescript KS^+ (see below). Unidirectional exonuclease III digestion (44) was then used to generate overlapping deletions which were sequenced from universal primer on single-stranded pBluescript KS^+ DNA templates. Both strands of the 4.7-kb *Hin*dIII fragment were sequenced. The *Kpn*I junction on plasmid pTA3 was verified by sequencing, using a synthetic oligonucleotide.

Plasmid constructions. The plasmids used for complementation studies in *E. coli* C600 $pyrBI_{1510}$ and for investigating the properties of recombinant ACTase are listed in Table 1. To generate these plasmids, the 4.7-kb *Hin*dIII fragment of pTA3 was first cloned in two orientations into pBluescript KS^+. From the resulting construct that carried the *pyr* gene cluster in sense orientation relative to the universal primer, a 1.9-kb fragment was removed by *Kpn*I digestion and self-ligation. This yielded plasmid pTAKS2.8S, which carries the *pyr* promoter, the *pyrR* gene, and the *pyrB* gene. The 1.9-kb *Kpn*I fragment itself was cloned in two orientations in pBluescript KS^+ to yield plasmids pTAKS1.9S and pTAKS1.9A, which carry *bbc* and gene *pyrC* in the sense and antisense orientations relative to the universal primer. From the pBluescript KS^+ construct that contained the 4.7-kb *Hin*dIII fragment with the *pyr* gene cluster in antisense orientation relative to the universal primer, a 2.8-kb *Kpn*I fragment was isolated and cloned into pBluescript KS^+, yielding plasmid pTAKS2.8A, which carries the same *pyr* genes as pTAKS2.8S but in the opposite orientation.

Plasmids pTAKS27, pTAKS26, and pTAKS25 were all constructed from pTAKS2.8S, by opening the latter plasmid with *Hin*dIII, protecting it with *Pst*I, treatment with exonuclease III and S1 nuclease, and blunt ending with the Klenow fragment of DNA polymerase, followed by ligation. Plasmid pTA3′, which contains gene *pyrB* and *bbc*, was constructed by subcloning the 1.8-kb *Bam*HI fragment from pTA3 into pUC18 (60).

Plasmids pTP1 and pTP1A carry the *Thermus pyr* promoter in the sense and antisense orientations, respectively, relative to a downstream located promoterless *cat* gene. These plasmids were constructed by cloning the 419-bp *Bam*HI fragment from pTAKS2.8S into promoter selection vector pKK232-8 (5).

All of these plasmids were initially constructed in *E. coli* TG1 by selecting for ampicillin resistance with 100 μg of ampicillin per ml. The structures of the plasmids were confirmed by restriction mapping, and those of pTAKS plasmids were also confirmed by sequencing. For expression studies, the pTA and pTAKS plasmids were transformed to *E. coli* C600 $pyrBI_{1510}$, and the pTP plasmids were transformed to *E. coli* JM101.

S1 mapping of the *pyr* promoter. S1 mapping was done essentially as described by Berk and Sharp (3). A 350-bp *Bam*HI fragment of pTAKS26, carrying the *Thermus pyr* promoter, was isolated from an agarose gel and treated with 20 U of calf intestinal phosphatase in 20 mM Tris-HCl (pH 9.5) for 30 min at 37°C. After phenol extraction and ethanol precipitation, dephosphorylated DNA was dissolved in 45 μl of denaturation buffer, incubated for 15 min at 50°C, and quickly chilled on ice; 5 μl of 10× kinase buffer was added, and the mixture was transferred to a dried [γ-^{32}P]ATP pellet (200 μCi). One microliter of T4 polynucleotide kinase was added; after a 40-min incubation at 37°C, the reaction was stopped with 150 μl of 2 M ammonium acetate. The DNA was ethanol precipitated in the presence of 25 μg of yeast tRNA. After *Sma*I digestion, a 301-bp 5′-labeled DNA fragment was recovered from a 6% polyacrylamide gel.

Extraction of *Thermus* strain ZO5 RNA was from a 1-liter culture (optical density at 650 nm of 0.5) which was suddenly cooled to 0°C by adding ice. Pelleted cells were resuspended in lysis buffer (pH 7.3) and lysed with lysozyme (3 mg) and sodium dodecyl sulfate (1%). Sodium acetate (pH 5.2, 100 mM) was added, and two acid phenol extractions (equal volumes) were carried out. RNA was ethanol precipitated (pH 8.0). The RNA pellet was dissolved in 5 ml of sterile water, freed of debris, and dialyzed in 2 liters of distilled water.

Fifty micrograms of *Thermus* strain ZO5 RNA or yeast tRNA and about 0.5 μg of ^{32}P-labeled fragment were precipitated with ethanol. The pellets were resuspended in 28 μl of deionized formamide, and 7 μl of salt mixture was added. Hybridizations and mock hybridizations were carried out at both 42 and 53°C for 3 h. To each tube, 350 μl of S1-containing buffer (200 U per ml) was added, and the reaction proceeded for 30 min at 45°C. The mixtures were precipitated, washed, and dried. Pellets were dissolved in 5 μl of formamide dye, boiled, and loaded on a denaturing sequencing gel. M13mp18 sequencing reactions with universal primer were used for size reference.

Enzyme assays. Exponentially growing cultures (200 ml) were harvested, washed, and sonicated, and the extracts were freed of cell debris as described previously (57). Recombinant ACTase was assayed in extracts of *E. coli* C600(pTA3, pTA3′, or pTAKS2.8) that had been cultured in minimal medium containing ampicillin. Chloramphenicol acetyltransferase (CAT) was assayed in extracts of *E. coli* JM101(pTP1 or pTP1A) that had been cultured in medium 853 containing ampicillin. ATCase and DHOase were assayed in extracts of *Thermus* strain ZO5 cultured in minimal medium D. The reaction temperatures were 37 and 55°C with *E. coli* and *Thermus* strain ZO5 extracts, respectively. ACTase activity was measured through the formation of carbamoylaspartate. The reaction mixture contained, in a total volume of 0.6 ml, 100 mM Tris-HCl (pH 8.25), 0 to 5 U of enzyme, 10 mM L-aspartate, and 5 mM carbamoyl phosphate. After 5 min of incubation, the reaction was stopped by adding 0.4 ml of 5% (wt/vol) trichloroacetic acid. Colorimetric measurement of carbamoylaspartate formed was done as described by Prescott and Jones (37). DHOase activities were also determined by measurement of the amount of carbamoylaspartate (37) produced during 5- to 10-min enzyme incubations. The standard DHOase assay was carried out with 0.025 to 0.2 ml of cell extract in the presence of 100 mM Tris-HCl (pH 8.25) and 3 mM dihydroorotate, with a final volume of 0.6 ml. Reactions were stopped by adding 0.4 ml of 5% trichloroacetic acid. CAT was assayed as de-

TABLE 1. Strains and plasmids used in this study

Strain or plasmid	Genotype or description	Source
Strains		
Thermus		
ZO5	Wild type, prototroph	This lab (10)
ZB1	*pyrB*	This study
E. coli		
TG1	*supE hsd*Δ*5 thi* Δ(*lac-proAB*) F′[*traD36 proAB*$^+$ *lacI*^{q}*lacZ*ΔM15]	
JM101	*supE thi* Δ(*lac-proAB*) F′[*traD36 proAB*$^+$ *lacI*^{q} *lacZ*ΔM15]	
C600 pyrBI$_{1510}$	Δ(*pro lac argF*)*argI*$^+$ *pyrBI*$_{1510}$ r$^-$ m$^-$	This lab
Plasmids and phagemids		
pUC18	Ap^r *lacZ*ΔM15, pBR322 ori[a]	Vieira and Messing (60)
pKK223-3	Ap^r, pBR322 ori	Brosius and Holy (6)
pKK232-8	Ap^r, pBR322 ori, promoterless *cat* gene	Brosius (5)
pBluescript KS$^+$	Ap^r *lacZ*ΔM15, ColE1 ori, M13 intergenic	Short et al. (50)
pTA3	pKK223-3 with 4.7-kb *Hin*dIII insert of *Thermus* strain ZO5 chromosome	This study
pTA3′	*Thermus* strain ZO5 *pyrB-bbc*; 1.8-kb *Bam*HI insert in pUC18	This study
pTAKS2.8S	*Thermus* strain ZO5 *pyrR-pyrB*; 2.8-kb *Hin*dIII-*Kpn*I insert in pBluescript KS$^+$ with orientation opposite that of β-galactosidase gene	This study
pTAKS2.8A	*Thermus* strain ZO5 *pyrR-pyrB*; 2.8-kb *Hin*dIII-*Kpn*I insert in pBluescript KS$^+$ with orientation identical to that of β-galactosidase gene	This study
pTAKS1.9S	*Thermus* strain ZO5 *bbc-pyrC*; 1.9-kb *Kpn*I-*Hin*dIII insert in pBluescript KS$^+$ with orientation opposite to that of β-galactosidase gene	This study
pTAKS1.9A	*Thermus* strain ZO5 *bbc-pyrC*; 1.9-kb *Kpn*I-*Hin*dIII insert in pBluescript KS$^+$ with orientation identical to that of β-galactosidase gene	This study
pTAKS27	pBluescript KS$^+$ with distal 1.88 kb of pTAKS2.8S	This study
pTAKS26	pBluescript KS$^+$ with distal 1.78 kb of pTAKS2.8S	This study
pTAKS25	pBluescript KS$^+$ with distal 1.52 kb of pTAKS2.8S	This study
pTP1	*Thermus* strain ZO5 *pyr* promoter; 419-bp *Bam*HI insert in pKK232-8, sense oriented relative to *cat* gene	This study
pTP1A	*Thermus* strain ZO5 *pyr* promoter; 419 bp *Bam*HI insert in pKK232-8, antisense oriented relative to *cat* gene	This study

[a] ori, origin of replication.

scribed by Shaw (48). Protein concentrations were determined by the Lowry method, with bovine serum albumin as a standard.

Nucleotide sequence accession number. The EMBL database accession number for the *Thermus* strain ZO5 *pyr* gene cluster is Y09536.

RESULTS

DNA sequence and functional identification of *pyr* genes. Recombinant plasmid pTA3, consisting of expression vector pKK223-3 and a unique 4.7-kb *Hin*dIII fragment of *Thermus* strain ZO5 DNA, complements an ATCase mutation in *E. coli* C600 pyrBI$_{1510}$, as previously reported (58). For this study, the nucleotide sequence of the 4.7-kb insert of pTA3 was determined on both strands, using the dideoxy-chain termination method (see Materials and Methods). A group of closely linked *pyr* genes was found on a 3.55-kbp subfragment. The locations, sizes, and order of detected genes are represented diagrammatically in Fig. 1. We identified, in order of transcription, *pyrR*, *pyrB*, an unidentified open reading frame (ORF) named *bbc* (between *pyrB* and *pyrC*), and *pyrC*. The gene-enzyme relationships, the enzyme subunit sizes, and calculated pI values are summarized in Table 2. The predicted amino acid sequence of *bbc* had no homolog in the protein databases.

The *Thermus* strain ZO5 *pyrR* gene was identified on the basis of deduced amino acid sequence similarities with *B. subtilis* and *B. caldolyticus pyrR*-encoded bifunctional proteins, which display weak UPRTase activity and play a role in the regulation of *pyr* gene expression (15, 30, 55). *Thermus* strain ZO5 *pyrR* exhibits 63.8, 56, and 47.4% identical residues with *pyrR* from *B. caldolyticus*, *B. subtilis*, and *Haemophilus influenzae*, respectively (13, 15, 55). Significantly weaker amino acid sequence identities, 19 and 27%, respectively, were seen with *E. coli* and *B. subtilis* UPRTase, encoded by the cognate *upp* genes (1, 31). On the basis of sequence similarities between a variety of phosphoribosyltransferases, Ghim and Neuhard proposed that residues 100 to 112 of *B. caldolyticus* PyrR constitute part of the PRPP binding site (15). Alignment of *Thermus* strain ZO5, *B. subtilis*, and *B. caldolyticus* PyrR amino acid sequences (Fig. 2) indicates that these residues are strongly conserved in *Thermus* PyrR (amino acids 99 to 111). In keeping with these results, purified *Thermus* PyrR protein displays UPRTase activity, catalyzing the formation of UMP from uracil and PRPP at high temperature (56). This enzyme may thus take part in a pyrimidine nucleotide salvage pathway in *Thermus* strain ZO5.

We have previously shown that *Thermus* strain ZO5 *pyrB* and *pyrC* genes are expressed in *E. coli* C600 pyrBI$_{1510}$(pTA3) and that recombinant ATCase and DHOase associate to form a 480-kDa multienzyme complex which is feedback inhibited by UTP (58). Purification of this complex and dissociation with KSCN yields inactive ATCase and an active 90-kDa DHOase which apparently consists of identical 45-kDa subunits (59). The latter estimated molecular mass agrees well with that predicted for the subunit of *Thermus* strain ZO5 DHOase on the basis of the DNA sequence of the *pyrC* gene (Table 2). *Thermus* strain ZO5 ATCase displays activity in vivo in the absence of DHOase, since plasmid pTAKS2.8S, which does

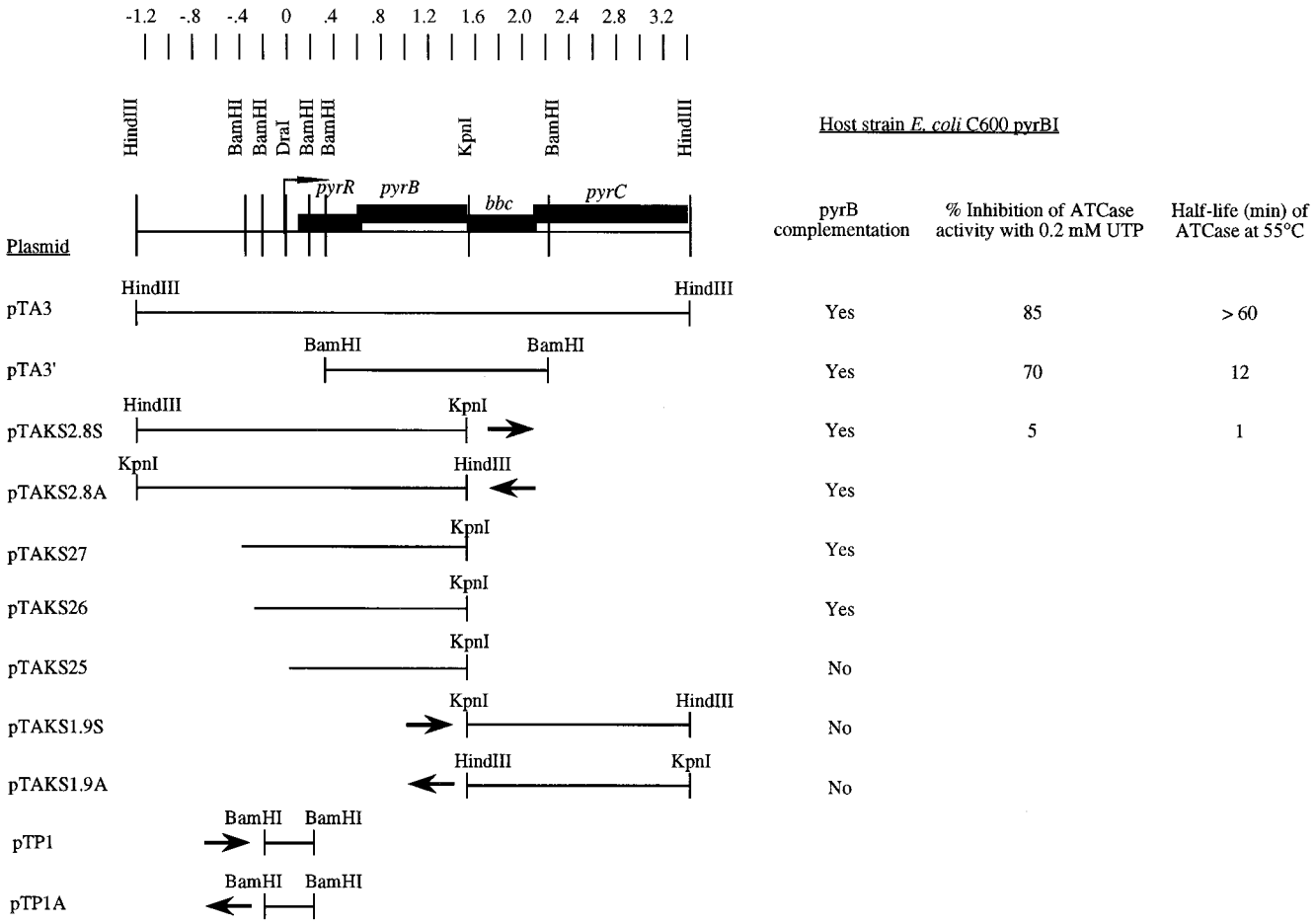

FIG. 1. Expression of full-length or truncated versions of the *pyr* gene cluster. The *Thermus* strain ZO5 *pyr* gene cluster is drawn schematically. Black boxes represent ORFs. Sizes (kilobase pairs) are indicated above the diagram; the arrow indicates the start point and direction of transcription. The structures of *E. coli* plasmids carrying different portions of the *Thermus pyr* gene cluster are represented below, with arrowheads indicating the sense direction. The growth of recombinant *E. coli* C600 $pyrBI_{1510}$ was tested on minimal medium 132 without uracil. Vigorous growth after 2 days of incubation at 37°C was taken as a positive result for *pyrB* complementation. Cell extracts of *E. coli*, in 50 mM Tris-HCl buffer (pH 8.25), were incubated at 55°C. At various time intervals, 100-μl aliquots were removed and chilled in a test tube containing the reaction mixture. The residual ATCase activity was then measured at 37°C (irreversible inactivation). The half-life of recombinant ATCase was determined by plotting the log of the residual activity versus time of heating. Feedback inhibition of *Thermus* ATCase was determined by assaying ATCase activity in extracts of recombinant *E. coli* at 37°C in the presence or absence of 0.2 mM UTP. Values indicate averages of two experiments with less than 20% variance.

not harbor *pyrC*, complements the ATCase mutation of *E. coli* C600 $pyrBI_{1510}$ (Fig. 1). In this case, ATCase consists only of catalytic subunits (*pyrB* encoded), and it is not inhibited by UTP (Fig. 1). Plasmid pTA3′ contains the 1.8-kbp *Bam*HI fragment carrying *pyrB* and *bbc*. The ATCase activity measured at 37°C in extracts of recombinant *E. coli* C600 $pyrBI_{1510}$(pTA3′) displayed feedback inhibition by UTP (Fig. 1). This negative control was slightly more pronounced in the ATCase-DHOase complex, expressed from plasmid pTA3 (Fig. 1). We also investigated the stability at 55°C of *Thermus* strain ZO5 ATCase formed in each of these genetic contexts. The results presented in Fig. 1 indicate that *Thermus* strain ZO5 ATCase was not stable in the absence of DHOase at temperatures compatible with *Thermus* growth. Therefore, thermal stability and regulation do not appear to be intrinsic properties of the *pyrB*-encoded catalytic chain. The data suggest that the *bbc*-encoded protein plays a role in feedback inhibition of ATCase. Whether this protein corresponds to an ATCase regulatory chain (a functional equivalent of the *E. coli* *pyrI* gene product) will require purification of active, UTP-regulated *Thermus* ATCase.

Amino acid sequence comparisons for enzymes encoded by *pyrB* and *pyrC*. The amino acid sequences deduced for *Thermus* ATCase and DHOase were compared and aligned to sequences available in the protein databases. Amino acid sequence identities were calculated from pairwise alignments created during a global homology search using the FASTA

TABLE 2. Summary of *Thermus* strain ZO5 Pyr enzyme structures, based on the deduced amino acid sequences

Gene	Enzyme	No. of amino acids	Mol wt	Calculated pI
pyrR	UPRTase	181	20,421	6.55
pyrB	ACTase	301	32,928	9.02
pyrC	DHOase	426	45,901	5.32
bbc	ATCase regulatory protein	194	20,786	10.80

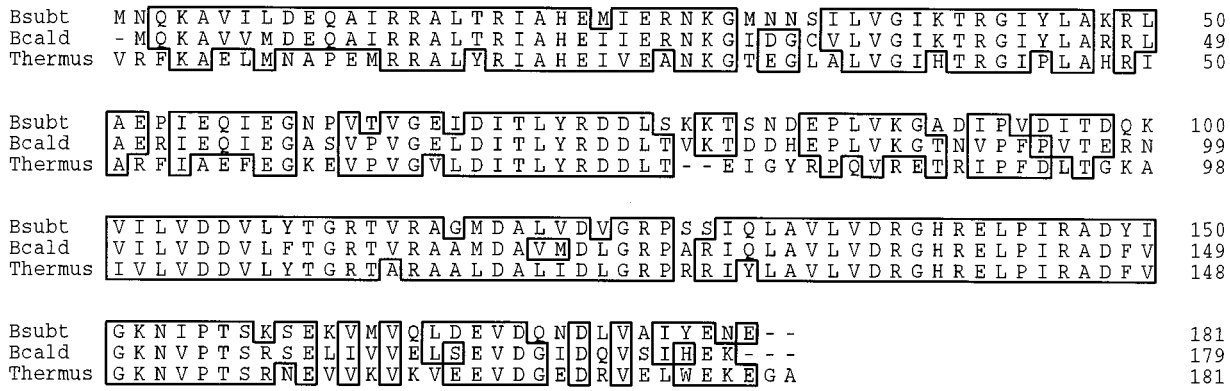

FIG. 2. Comparison of the deduced amino acid sequence of *Thermus* strain ZO5 PyrR (Thermus; this work) with sequences of the *pyrR*-encoded UPRTases from *B. subtilis* (Bsubt) and *B. caldolyticus* (Bcald). Identical and similar amino acids are boxed. Dashes denote gaps. Sequence numberings (right) for *B. subtilis* and *B. caldolyticus* PyrR are according to their Swiss_Prot accession numbers, P25982 and P41007, respectively.

program from the University of Wisconsin Genetics Computer Group (GCG) package (11).

The predicted amino acid sequence of the Thermus strain ZO5 *pyrB* ORF exhibits greater similarities with *P. aeruginosa* (50.2% amino acid identity) and *P. putida* ATCase (49.3% identity) than with the ATCases from *B. caldolyticus* (42.7% identity) and *B. subtilis* (39.8%). Sequence identities with *E. coli* ATCase and with the ATCase domain in the hamster or yeast carbamoyl phosphate synthetase-ATCase-DHOase multifunctional proteins (CAD proteins) ranged from 31 to 35%.

For the translated *Thermus pyrC* ORF, the highest similarity scores were seen with DHOase from *B. caldolyticus* and *B. subtilis* (44.4 and 39.2% identity, respectively). *Thermus* strain ZO5 DHOase is also homologous to the DHOase domain in the CAD protein of hamster (38.8% identity) as well as the *pyrC′*-encoded DHOase-like proteins of *P. aeruginosa* and *P. putida* (35.1 and 32.5% identity). Lower scores were obtained with *E. coli* DHOase and the inactive yeast CAD protein (24.9 and 21.0% identity).

The predicted *Thermus* strain ZO5 ATCase and DHOase amino acid sequences were aligned to other homologous sequences by using the PILEUP GCG program (Fig. 3 and 4, respectively). In these alignments, the most related sequences are immediately superimposed. *Thermus* ATCase appears most closely related to ATCases from *P. aeruginosa* and *P. putida* but does not possess the 11-amino-acid PyrI-like N-terminal extension (Fig. 3) which provides the ATP nucleotide effector binding site in the *Pseudomonas* enzymes (2, 26, 47). Of the 16 amino acids contributing to the active site of *E. coli* ATCase, 13 are conserved at corresponding positions in *Thermus* strain ZO5 ATCase (Fig. 3). Multiple sequence alignment and comparison of *Thermus* strain ZO5 DHOase with seven other DHOases indicates that few residues are conserved in all sequences (Fig. 4). Five histidine residues thought to be involved in Zn^{2+} binding (39, 51) are conserved in DHOases from *B. subtilis*, *B. caldolyticus*, *E. coli*, hamster, and *Thermus* strain ZO5 (Fig. 4). Other putative components of the active site in *E. coli* DHOase are Met-43, Pro-44, Asn-45, Asp-251, Ser-252, Ala-253, Pro-254, His-255, and Lys-260 (47, 51). With the exception of Ser-252, all of these residues are also found at corresponding positions in *Thermus* strain ZO5 DHOase. Ser-252 of *E. coli* DHOase is replaced by a His residue in the *Bacillus* and *Thermus* strain ZO5 enzyme sequences (Fig. 4). The positional identity between DHOases from *B. subtilis* and *Thermus* strain ZO5 attains 39%, which is in line with the level of identity between the cognate ATCases.

Gene organization. The translational start sites for *Thermus pyr* genes were predicted from the nucleotide sequence and by comparison of the deduced amino acid sequences to homologous proteins; corresponding ATG or GTG codons were about 5 nucleotides (nt) downstream from sequences that resemble stable ribosome binding sites. Table 3 shows the sequences surrounding the predicted translation start sites, the deduced ribosome binding sites, and the predicted ΔG values (53) for base pairing between the 3′ end of *T. thermophilus* 16S rRNA (19) and the ribosome binding sites. The predicted ΔG values for these interactions range from −14.5 to −21 kcal/mol, averaging −17.7 kcal/mol. The ΔG values for *pyr* genes in *B. subtilis* average −15 kcal/mol (39).

The 3′ end of the *pyrR* ORF and the 5′ end of the *pyrB* ORF overlap by 4 nt, as do the 3′ end of *bbc* and the 5′ end of the *pyrC* ORF. *pyrB* and *bbc* are separated by 1 nt, but the TGA stop codon of *pyrB* is part of the proposed ribosome binding site of *bbc* (Table 3).

In *B. caldolyticus* and *B. subtilis*, the *pyrR*, *pyrP*, and *pyrB* genes are separated by 150- to 200-nt intercistronic regions, but in *Thermus*, the *pyrR* and *pyrB* genes are joined (Table 3), and the equivalent of *pyrP*, encoding a uracil permease in *Bacillus* sp. (15, 55), was not found (Fig. 1). In *Bacillus* sp., the *pyrB* and *pyrC* genes overlap, as do the *pyrB* and *pyrC′* genes in *Pseudomonas* (16, 39, 47); however, in *Thermus* strain ZO5, *bbc* lies between *pyrB* and *pyrC* (Fig. 1). The *Thermus pyr* gene cluster described here contains four closely linked ORFs and probably encodes a polycistronic message. Whether other pyrimidine biosynthesis genes are located immediately downstream of *pyrC*, as is the case in *Bacillus* sp., cannot be decided on the basis of the presently available sequence data.

The overall GC content of the *Thermus pyrR*, *pyrB*, and *pyrC* genes averages 69%, which is in line with the genomic GC content of *T. thermophilus* (35). The codon usage in these genes is strongly biased toward the use of G or C in the first (±72%) and third (±92%) codon positions; the GC frequency in the second codon positions (±42%) is comparatively low. The bias for codons starting or ending in G or C is reflected in the amino acid compositions of *pyr* gene-encoded proteins in *Thermus* strain ZO5 and to a lesser extent in *B. caldolyticus* (Table 4). The arginine content of ATCase and DHOase increases gradually from *B. subtilis* to *B. caldolyticus* to *Thermus*

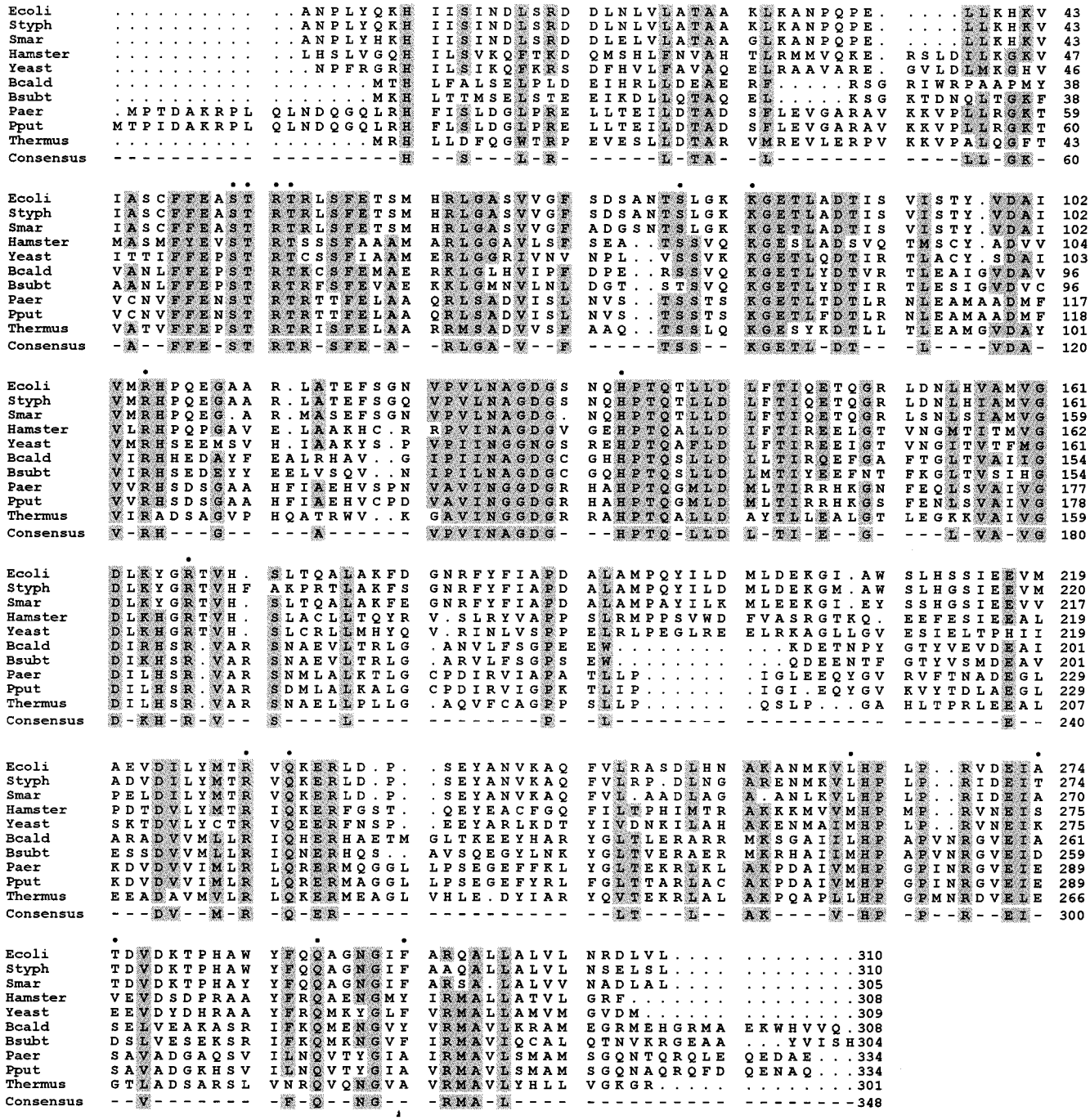

FIG. 3. Comparison of the deduced amino acid sequence of *Thermus* strain ZO5 PyrB with sequences of ATCases from *E. coli* (Ecoli; accession no. P00479), *Salmonella typhimurium* (Styph; P08420), *Serratia marcescens* (Smar; P19910), hamster (P08955), yeast (P07259), *B. caldolyticus* (Bcald; P41008), *B. subtilis* (Bsubt; P05654), *P. aeruginosa* (Paer; L19649), and *P. putida* (Pput; A56144). Amino acid sequences were retrieved from the protein databases (according to the sequence accession numbers indicated above) and aligned by using the PILEUP GCG program. Identical and similar amino acids are indicated by shaded boxes. Known active-site residues in *E. coli* ATCase are indicated (●). The consensus indicates residues identical in 6 of 10 sequences. Dots denote gaps. Sequence numbering is on the right.

strain ZO5. Similarly, an increased number of prolines and leucines is observed in the *Thermus* strain ZO5 enzymes (Table 4). A closer inspection suggests that the increases in arginine (CGX) and in leucine ([U/C]UX) or proline (CCX) are largely at the expense of the related amino acids lysine (AAX) and isoleucine (AUX), respectively. The tendencies observed probably reflect, at least in part, variations in genomic GC content. However, it is possible that some of these amino acid exchanges contribute to the stability or mutual stabilization of thermophilic *pyr* enzymes (22, 23, 32, 34, 40, 62). The observed substitutions cannot be interpreted without any additional information regarding the protein three-dimensional structures.

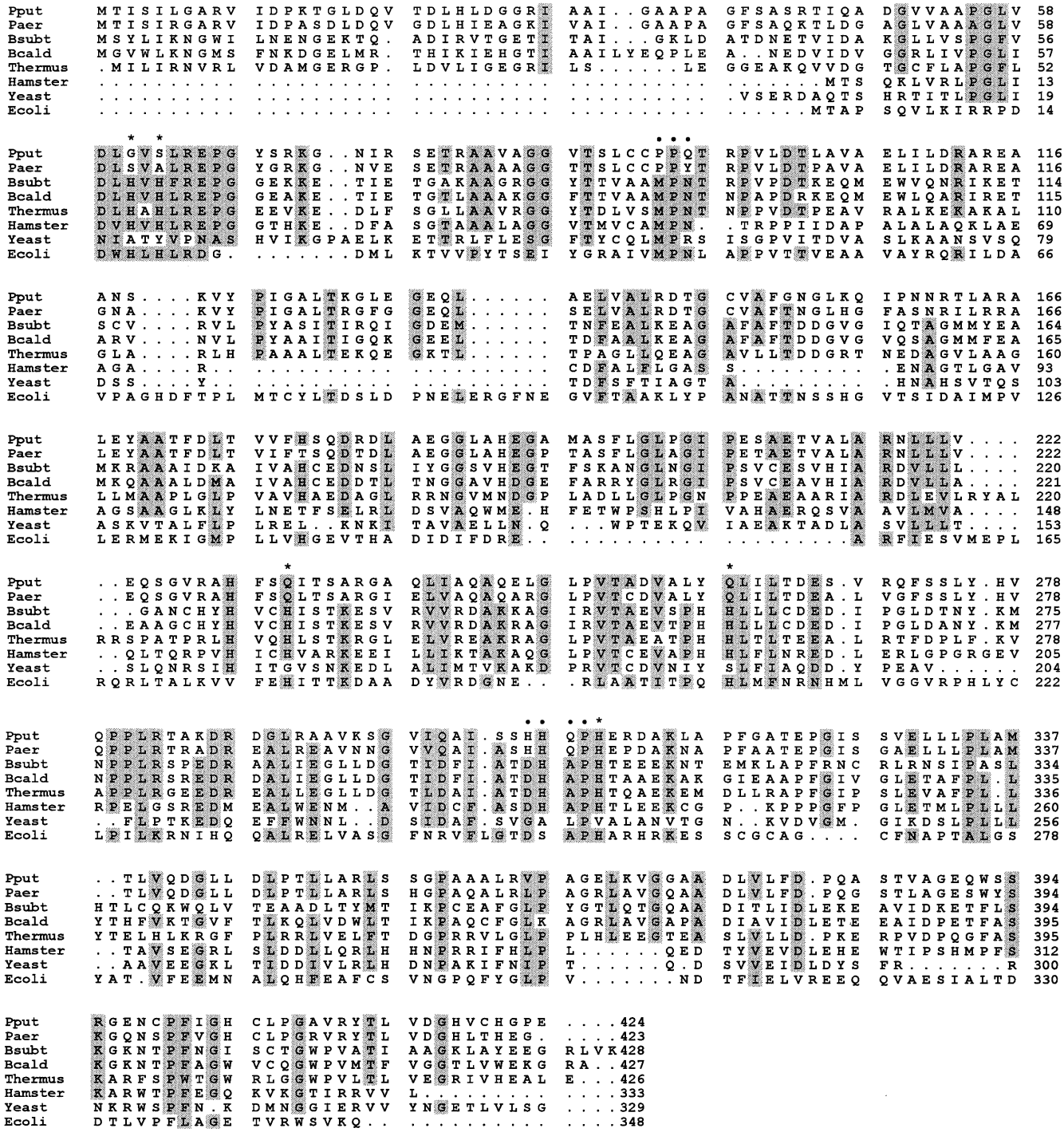

FIG. 4. Comparison of the deduced amino acid sequence of *Thermus* strain ZO5 *pyrC* with sequences of known DHOases. The amino acid sequences of *P. putida* (Pput; accession no. B56144), *P. aeruginosa* (Paer; L19649), *B. subtilis* (Bsubt; P25995), *B. caldolyticus* (Bcald; P46538), *Thermus* strain ZO5 (Thermus; this work), hamster (P08955), yeast (P07259), and *E. coli* (Ecoli; P05020) were aligned. Identical and similar residues are indicated by shaded boxes. Putative active site residues of *E. coli* DHOase are indicated (●); five conserved histidine residues assumed to be important for Zn^{2+} binding are marked (*). Other details are as for Fig. 3.

Promoter identification and function. The transcription initiation site for *Thermus* strain ZO5 *pyr* gene cluster mRNA was determined by S1 nuclease mapping using RNA isolated from *Thermus* cells grown on 162 AUF medium (see Materials and Methods) and a 5′ ^{32}P-labeled probe constructed as shown in Fig. 5A. This finding indicated that transcription initiation occurs in the vicinity of a pair of guanine residues located 6 bases downstream of the putative −10 element of the promoter sequence TTGCCGN$_{17}$TAAGGTA (Fig. 6). The *Thermus* strain ZO5 *pyr* promoter resembles other previously reported *Thermus* promoters (12, 25, 33, 46) and also conforms to the *E. coli* promoter consensus (20, 43). The results of

TABLE 3. Translation start sites, ribosome binding sites, and overlap of reading frames for polypeptides encoded in the *Thermus* strain ZO5 *pyr* gene cluster[a]

Sequence	ΔG (kcal/mol)	No. of overlapping residues with preceding gene
Met-leader CCGAAAGGGGGAGAGATGCGAGAAACAAGGAAGCG	−15	None
Met-*pyrR* TTTGGAGGTGGCCGGTGCGCTTTAAGGCGGAGCTC Stop-leader	−19.1	11
Met-*pyrB* GGAAAAGGAGGGGGCATGAGGCACCTCCTGGACTT Stop-*pyrR*	−19	4
Met-*bbc* AAAAGGGAGGTGACGTGGGGTACCATGAGGCCATG Stop-*pyrB*	−21	None, 1 bp intercistronic
Met-*pyrC* AACTGGAGGAACGATGATCCTGATCCGAAACGTAC Stop-*bbc*	−14.4	4

[a] The sequences shown are located around translation initiation sites for the leader peptide, UPRTase (*pyrR* gene), ATCase (*pyrB* gene), the *bbc* ORF, and DHOase (*pyrC* gene). Overlining indicates complementarity to the 3′ end of the *T. thermophilus* 16S rRNA, 3′UCUUUCCUCCACUAG (19). The rules of Tinoco et al. (53) were applied to calculate the free energy for binding for the 16S rRNA and the putative ribosome binding sites. The start codon for each gene is underlined and indicated above the DNA sequence by Met-gene. The termination codon for an overlapping reading frame is underlined and indicated below the sequence by Stop-gene.

complementation experiments with pBluescript-based plasmids pTAKS2.8S and pTAKS2.8A (Fig. 1) already suggested that expression of the *Thermus pyr* genes in *E. coli* did not rely on a vector-borne promoter. Moreover, progressive removal of DNA sequences upstream of *pyrR* in plasmids pTAKS27 and pTAKS26 (Fig. 1) did not interfere with *pyr* gene expression (*pyrB*), unless the deletion included the *Thermus pyr* promoter, as in pTAKS25 (Fig. 1). Furthermore, subcloning of a 419-bp *Bam*HI fragment carrying the *Thermus pyr* promoter into the promoter reporter vector pKK232-8 yielded a high CAT level (126 nmol min^{-1} mg^{-1}) in *E. coli* and supported growth in the presence of 400 μg of chloramphenicol per ml when the *pyr* promoter was in the sense orientation relative to the downstream *cat* gene (pTP1 [Fig. 1]). The *pyr* promoter functioning in the antisense direction (pTP1a [Fig. 1]) did not yield a detectable CAT activity, nor did it support growth of *E. coli* in the presence of 50 μg of chloramphenicol per ml. These results strongly suggest that the *Thermus* strain ZO5 *pyr* promoter identified here also functions in *E. coli*.

Transcription signals. The *Thermus* strain ZO5 *pyr* promoter is separated from the translation initiation site of the *pyrR* gene by 120 nt. Structurally, this promoter region (Fig. 6) is characterized by (i) a putative rho-independent terminator sequence ($\Delta G = -24.6$ kcal/mol [53]) centered about +88; (ii) two potential ribosome binding sites with sequences complementary to the 3′ end of 16S rRNA, indicated as SD1 (leader [Table 3]) and SD2 (*pyrR* [Table 3]); (iii) a potential leader polypeptide of 28 amino acids, initiating translation at +41; (iv) a 40-nt-long presumptive RNA-binding protein recognition site between +1 and +41, conforming to the consensus of three sequences (Fig. 7) which were found to overlap antiterminators in different intercistronic regions along the *pyr* operon in *B. caldolyticus* and *B. subtilis* (14, 15, 29, 55) and to bind the PyrR protein (30); (v) the absence of an antiterminator-like structure or other predictable secondary RNA structure upstream of the rho factor-independent terminator when the FOLD GCG program (11, 65) was used to screen this region; and (vi) an overlap between the putative *pyrR*-regulatory protein binding site and the potential leader ribosome binding site SD1 (Fig. 6).

Regulation of pyrimidine gene expression. Specific activities of ATCase and DHOase were measured at 55°C in cell extracts of *Thermus* strain ZO5 exponentially grown at 65°C in minimal medium D and in medium D containing uracil (50 μg/ml) or arginine (100 μg/ml). As shown in Table 5, addition of uracil resulted in about threefold reduction of *pyrB* and *pyrC* expression. In contrast, addition of arginine increased *pyrB* and *pyrC* expression twofold (Table 5). The data obtained for arginine and uracil illustrate that *pyr* gene expression in *Thermus* strain ZO5 is modulated over at least a sevenfold range. A *Thermus* strain ZO5 *pyrB* mutant strain which lacks ATCase activity, *Thermus* strain ZB1 (Table 1), was grown in minimal medium D containing 4 μg of uracil per ml. Upon reaching the station-

TABLE 4. Predicted amino acid compositions of three Pyr proteins from *Thermus* strain ZO5, *B. caldolyticus*, and *B. subtilis*[a]

Amino acid	Occurrence of amino acid								
	UPRTase			ATCase			DHOase		
	Th	Bc	Bs	Th	Bc	Bs	Th	Bc	Bs
Ala	17	13	12	36	31	17	49	56	43
Cys		1		1	2	3	**1**	**7**	**10**
Asp	12	15	17	13	12	14	23	26	24
Glu	18	14	12	21	31	29	39	33	34
Phe	5	3		7	11	11	11	16	11
Gly	14	12	11	21	21	19	41	41	35
His	4	4	2	8	15	9	13	15	13
Ile	13	16	19	**6**	**18**	**17**	**8**	**26**	**30**
Lys	8	7	11	11	10	16	**14**	**21**	**27**
Leu	18	16	17	**42**	**28**	**27**	**73**	**36**	**34**
Met	2	4	4	8	11	10	6	11	10
Asn	4	4	8	5	7	14	7	10	18
Pro	8	7	7	**16**	**12**	**6**	**35**	**20**	**19**
Gln	1	5	7	13	6	14	6	9	9
Arg	**21**	**18**	**13**	**25**	**29**	**17**	**33**	**20**	**18**
Ser	1	5	7	15	13	25	9	7	17
Thr	9	10	10	16	16	22	24	30	36
Val	20	23	18	29	24	25	28	31	26
Trp	1			2	3	1	3	6	4
Tyr	5	2	5	6	8	8	3	6	10

[a] The occurrence of a particular amino acid is indicated for each enzyme. Th, *Thermus* strain ZO5; Bs, *B. subtilis*; Bc, *B. caldolyticus*; *B. subtilis* and *B. caldolyticus* sequences are from references 39 and 16, respectively. Tendencies discussed in the text are in boldface.

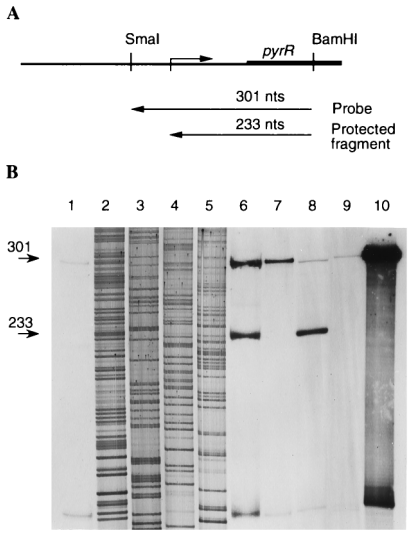

FIG. 5. S1 nuclease mapping of *Thermus* strain ZO5 *pyr* mRNA upstream of *pyrR*. (A) Drawing depicting the probe used and the fragment protected by mRNA extracted from *Thermus* strain ZO5 cells. The probe was single stranded, 5′ labeled with [γ-^{32}P]dATP, and complementary to *pyr* mRNA at its proximal (5′) end. The single-stranded probe was derived from a double-stranded labeled *Bam*HI-*Sma*I fragment by denaturation at 90°C for 10 min prior to annealing. (B) Autoradiogram using the probe described. The GATC sequencing lanes 2 to 5 were generated by sequencing an M13mp18 control template with the universal −20 primer. The numbers on the left are sizes (in nucleotides) determined from the sequencing. Lane 1, 50 μg of yeast tRNA annealed with the probe before digestion with S1 nuclease (negative control); lane 10, control omitting S1 nuclease; lane 6, probe annealed at 42°C with 50 μg of RNA extracted from *Thermus* strain ZO5 grown in 162 AUF medium; lane 7, probe annealed at 42°C with 50 μg of yeast tRNA; lane 8, probe annealed at 53°C with 50 μg of *Thermus* strain ZO5 RNA prepared as for lane 6; lane 9, probe annealed with 50 μg of yeast tRNA at 53°C. Annealing was 3 h at the mentioned temperatures before digestion with S1 nuclease for 30 min at 37°C.

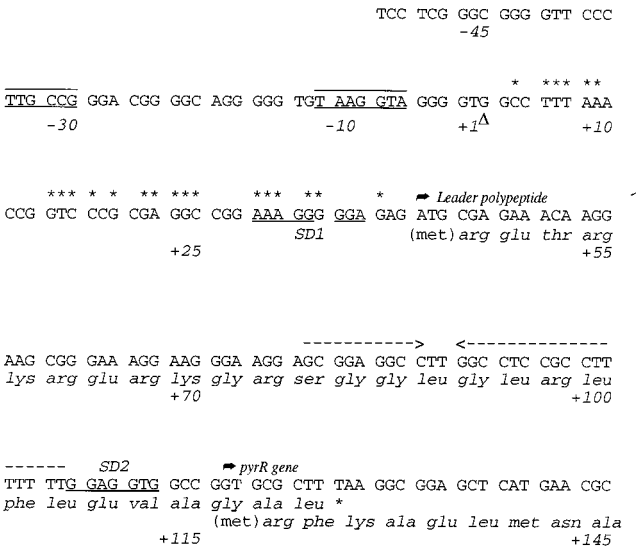

FIG. 6. Characteristics of the *pyr* initiation region. The location of the major transcriptional initiation region is indicated by a triangle and orients the sequence from +1. The −10 and −35 promoter elements are sandwiched between lines. Two possible ribosome binding sites are indicated as SD1 at +29 and SD2 at +106. A possible leader initiation codon (ATG) lies downstream of SD1 at +41, and the presumptive translational initiation site (GTG) for *pyrR* is indicated at +117. The leader polypeptide (28 amino acids) is indicated with an italicized amino acid sequence deduced from the DNA sequence which extends 11 nt into the *pyrR* ORF; the stop codon is marked by an asterisk below the DNA sequence. The amino terminus of *pyrR* begins in a different reading frame with *arg*, *phe*, and *lys* at +120. A strong rho factor-independent terminator is indicated by broken arrows from +78 to +105. Asterisks above the DNA sequence mark a region of sequence conservation with the *Bacillus* consensus for *pyr*-regulatory protein binding (Fig. 7).

ary phase (optical density at 650 nm of 0.3), the cells were starved for pyrimidines during a 3-h period and DHOase specific activity was determined. The data in Table 5 indicate that upon pyrimidine starvation, the expression level of *pyrC* increased about fourfold. Collectively, the results indicate that expression of the *pyr* gene cluster in *Thermus* strain ZO5 is antagonistically regulated by pyrimidines and arginine.

DISCUSSION

In this study, we sequenced a 4.7-kbp fragment of *Thermus* strain ZO5 DNA that complements an ATCase mutation in *E. coli*, disclosing the existence of a pyrimidine gene cluster in *Thermus*. This cluster is expressed in *E. coli* from its native promoter and encodes two *pyr* biosynthetic activities (*pyrB* and *pyrC*) and the pyrimidine pathway salvage enzyme UPRTase (*pyrR*). We have shown that in *Thermus* strain ZO5, the level of de novo enzymes ATCase (*pyrB*) and DHOase (*pyrC*) is threefold repressed by uracil and twofold increased by arginine. In a *Thermus* strain ZO5 *pyrB* mutant, exhaustion of pyrimidines led to fourfold derepression of *pyrC* (Table 5). On the basis of gene organization and predicted amino acid sequences, the *Thermus pyr* gene cluster resembles the proximal part of the *B. caldolyticus* and *B. subtilis pyr* operons. In these organisms, transcription of *pyr* genes is also controlled by the availability of pyrimidines, and this was recently shown to occur via an attenuation mechanism (14–16, 29, 55). There are three transcription terminators within the *Bacillus pyr* operons, each of which is preceded by another stem-loop structure, the antiterminator, whose formation would prevent formation of the terminator stem-loop. These structures are found in the untranslated leader, in the *pyrR-pyrP* intercistronic region, and in the *pyrP-pyrB* intercistronic region. In *Bacillus* sp., the PyrR protein binds to conserved sequences in *pyr* mRNA and disrupts the antiterminators, promoting transcription termination when pyrimidine nucleotides are abundant (29, 30, 55). An equivalent of the *Bacillus pyrP* gene surrounded by two intercistronic regions was not found in the *Thermus* strain ZO5 *pyr* gene cluster. Nevertheless, the *Thermus pyr* transcript contains one rho factor-independent terminator structure ($\Delta G = -24.6$ kcal/mol) located upstream of the *pyrR* gene, as in *Bacillus*. We could not identify any antiterminator-like or other predictable RNA secondary structure upstream of this terminator. However, alignment and comparison of the deduced amino acid sequence of *Thermus* strain ZO5 PyR with the *pyrR*-encoded regulatory proteins of *B. subtilis* and *B. caldolyticus* suggests a role for *Thermus* PyrR in the regulation of *pyr* gene expression (Fig. 2). Moreover, we found a DNA sequence in the *Thermus pyr* promoter region that conforms to the consensus recognition site for the *B. subtilis* and *B. caldolyticus pyrR* attenuation proteins (Fig. 7), which were proposed to complex mRNA specifically when bound to a pyrimidine effector (probably UMP). In *Thermus* strain ZO5, this presumptive *pyrR* binding site overlaps the ribosome binding site SD1 of the leader (Fig. 6). We therefore propose that, in the regulated expression of the *Thermus* strain ZO5 *pyr* gene cluster, the role of the *Bacillus* antiterminator may be played by a leader-translating ribosome precluding formation of the transcription terminator. The binding of *Thermus* PyrR at its proposed recognition site in the transcript would prevent initiation of translation of the

Organism	Region		Sequence	
B. caldolyticus	promoter-*pyrR*	12	AACC**UUUAA**GUUC**AGUCC**U**GU**G**AGGCU**GAA**AA**GG**GG**UCGGA**AU**	54
	pyrR-pyrP	702	CCC**UUUUAA**GCGC**AGUCCC**G**U**G**AGGCU**GCA**AAA**GG**GG**CGG**AA**U**	744
	pyrP-pyrB	2163	ACC**UUUUAA**-UUA**AGUCCC**G**C**G**AGGCU**UAA**AAA**GG**GU**GUGA**AA**A**	2204
B. subtilis	promoter-*pyrR*	9	GAU**U**C**UU**U**A**AAAC**AGUCC**A**GA**G**AGGCU**GAG**AA**GG**A**UAACGG**AU**	51
	pyrR-pyrP	704	CCU**UUUUAA**GGGC**AA**U**CC**A**GA**G**AGG**U**U**GC**A**AA**GA**G**GU**GC**AC**AA**	746
	pyrP-pyrB	2176	ACC**UUUUAA**UGAA**AGUCC**A**GA**G**AGGCU**UGG**AA**GG**GU**UAU**GA**AG**	2218
Bacillus	consensus		**...UUUUAA....AGUCC.G.GAGGCU...AA.GG.....A.**	
Thermus ZO5	promoter-*pyrR*	1	GGCC**UUUAAA**-CCG**GUCCC**G**C**G**AGGC**CGGA**AA**GG**GG**GAGA**G**AU**	42

FIG. 7. Alignment of the *Thermus* strain ZO5 *pyr* promoter region with a consensus for six putative *pyrR* binding sites found in the *B. caldolyticus* and *B. subtilis* *pyr* operons (14, 15, 29). Bases that are marked boldface were identical in five of six *Bacillus* sequences and were taken for the consensus. Dots indicate no consensus for that position. Bases that are marked boldface in the *Thermus* strain ZO5 sequence are identical to those in the *Bacillus* consensus. Numbers indicate nucleotide positions in the respective transcripts.

leader peptide, resulting in terminator formation and reduced expression of the downstream located *pyr* genes when pyrimidine nucleotides are abundant. Furthermore, according to this model, the positive effect an excess arginine has on pyrimidine gene expression may result from enhanced translation of the arginine-rich leader peptide (20% arginine residues) compared to when this amino acid is absent from the medium. Molecular studies on regulation of *Thermus pyr* gene expression are in progress in our laboratory; the PyrR protein has been overexpressed and purified in order to investigate in vitro whether the attenuation mechanism that we propose here is functional. We will investigate whether the PyrR protein binds to its proposed target sequence and which nucleotide effectors this may involve.

The *Thermus* strain ZO5 PyrB polypeptide is stable at 55°C only when the *pyrC* gene is also expressed (Fig. 1), suggesting that *Thermus* ATCase is stabilized, at least in part, by binding DHOase. This is in agreement with our recent finding that recombinant ATCase and DHOase can be partially purified as a thermostable 480-kDa multienzyme complex (58, 59). Several observations suggest that the translation product of gene *bbc* is responsible for UTP feedback inhibition of *Thermus* strain ZO5 ATCase and that it participates in the multipeptide complex. First, expression of *pyrB* in the presence of *bbc* gives an ATCase which is strongly feedback inhibited by UTP, whereas expression of the *pyrB* gene alone yields an unregulated ATCase (Fig. 1). Second, the *bbc* translation product apparently also stabilizes ATCase partially (Fig. 1). Third, we have shown that progressive purification of the recombinant ATCase-DHOase complex results in loss of the regulatory properties (UTP inhibition), while the two enzyme activities remain intact (59). This also suggests the involvement of rather loosely associated regulatory subunits. Since we did not succeed in purifying to homogeneity the regulated multienzyme complex, we have no data at present, other than the 480 kDa estimated from molecular sieving (58), from which to evaluate directly the stoichiometry for *pyrB*, *pyrC*, and *bbc* subunits in the complete structure.

The complementations obtained in an *E. coli pyrB* mutant with plasmids pTAKS2.8S and pTA3′ indicate that both the unregulated and regulated (with *bbc*) forms of *Thermus* ATCase are active in the absence of *Thermus* DHOase. That these two types of ATCase would have to form a complex with *E. coli* DHOase to yield the observed complementations is unlikely for the following reasons. First, there is no evidence in the literature for protein-protein interactions between *E. coli* ATCase and DHOase or between *E. coli* DHOase and any other enzyme. Second, the amino acid sequence similarity between *Thermus* DHOase and *E. coli* DHOase (24.9%) is among the weakest observed for DHOase. Third, our results indicate that *Thermus* ATCase is very labile in extracts containing *E. coli* DHOase but not in extracts also containing *Thermus* DHOase (Fig. 1). Furthermore, molecular sieving did not reveal a possible association between *Thermus* ATCase and *E. coli* DHOase; recombinant *Thermus* ATCase was completely inactivated during gel filtration of extracts that contained *E. coli* DHOase but not *Thermus* DHOase (not shown). Hence, as the complementation experiments indicate, *Thermus* ATCase can be active without DHOase at 37°C, unlike *Pseudomonas* ATCase, which requires DHOase-like proteins to remain active (2, 47). In addition to its catalytic role, *Thermus* DHOase apparently also plays a vital role in stabilizing the ATCase at extreme temperature.

High-M_r (450,000 to 500,000) proteins with ATCase activity and composed of polypeptides of around 34 and 45 kDa are widely distributed in the bacterial domain (24). This so-called class A type of ATCase has been encountered within the γ subdivision of the proteobacteria: in three fluorescent pseudomonads, in *Azomonas agilis*, and in *Azotobacter vinelandii*. A class A type of ATCase was also found in *Paracoccus denitrificans*, a species belonging to the α subdivision of the proteobacteria (24). Furthermore, a 500-kDa ATCase was found in *Deinococcus radiophilus* (24), which on the basis of its 16S rRNA sequence, is phylogenetically remote from the proteobacteria while being closely related to *Thermus* sp. (63). At present, it is not known whether *D. radiophilus* ATCase forms a multienzyme complex with an active DHOase (48a); however, the existence of a *pyr* enzyme cluster in *Thermus*, a thermophilic member of the rather deeply branching *Deinococcus*/*Chloroflexus* group, raises the possibility that ATCase-DHOase multifunctional complexes are more widespread than is presently perceived.

TABLE 5. Pyrimidine biosynthesis enzyme activities in *Thermus* strain ZO5

Organism *Thermus* strain	Growth condition	Sp act at 55°C (μmol h^{-1} mg^{-1})[a]	
		ATCase	DHOase
ZO5	Medium D	1.18 ± 0.22	0.53 ± 0.07
	Medium D + uracil	0.33 ± 0.06	0.16 ± 0.05
	Medium D + arginine	2.44 ± 0.23	1.04 ± 0.03
ZB1	Medium D + 4 μg of uracil/ml		0.14 ± 0.03
	Medium D, uracil starvation		0.59 ± 0.05

[a] Average of four independent experiments ± SD.

ACKNOWLEDGMENTS

This work was supported by a Concerted Action between the Vrije Universiteit Brussel and the Belgian state, by the Belgian Fund for Joint Scientific Research, and by the Vlaams Instituut voor de bevordering van het Wetenschappelijk-Technologisch onderzoek in de industrie.

REFERENCES

1. **Andersen, P. S., J. M. Smith, and B. Mygind.** 1992. Characterization of the *upp* gene encoding uracil phosphoribosyltransferase of *Escherichia coli* K12. Eur. J. Biochem. **204:**51–56.
2. **Berg, S. T., and D. R. Evans.** 1993. Subunit structure of class A aspartate transcarbamoylase from *Pseudomonas fluorescens*. Proc. Natl. Acad. Sci. USA **90:**9819–9822.
3. **Berk, A. J., and P. A. Sharp.** 1977. Sizing and mapping of early adenovirus mRNAs by gel electrophoresis of S1 endonuclease-digested hybrids. Cell **12:**721–732.
4. **Blank, J., S.** 1994. EMBL/GenBank/DDBJ database submission, accession no. X83598; Swiss-Prot, PYRH_THETH, P43891.
5. **Brosius, J.** 1984. Plasmid vectors for the selection of promoters. Gene **27:**151–160.
6. **Brosius, J., and A. Holy.** 1984. Regulation of ribosomal RNA promoters with a synthetic *lac* operator. Proc. Natl. Acad. Sci. USA **81:**6929–6933.
7. **Castenholz, R. W.** 1969. Thermophilic blue-green algae and the thermal environment. Bacteriol. Rev. **33:**476–504.
8. **Clemmesen, K., F. Bonenkamp, O. Karlstrom, and K. F. Jensen.** 1985. Role of translation in the UTP-modulated attenuation at the *pyrBI* operon of *Escherichia coli*. Mol. Gen. Genet. **201:**247–251.
9. **Davidson, J. N., and M. E. Wales.** 1996. Alignment of aspartate transcarbamylase sequences. Paths Pyrimidines **April:**11–17.
10. **Degryse, E., N. Glansdorff, and A. Piérard.** 1978. A comparative analysis of extreme thermophilic bacteria belonging to the genus *Thermus*. Arch. Microbiol. **117:**189–196.
11. **Devereux, J., P. Haeberli, and O. Smithies.** 1984. A comprehensive set of sequence analysis programs for the VAX. Nucleic Acids Res. **12:**387–395.
12. **Faraldo, M. M., M. A. de Pedro, and J. Berenguer.** 1992. Sequence of the S-layer gene of *Thermus thermophilus* HB8 and functionality of its promoter in *Escherichia coli*. J. Bacteriol. **174:**7458–7462.
13. **Fleischmann, R. D., M. D. Adams, O. White, R. A. Clayton, et al.** 1995. Whole-genome random sequencing and assembly of *Haemophilus influenzae* Rd. Science **269:**496–512.
14. **Ghim, S.-Y., and R. L. Switzer.** 1996. Characterization of *cis*-acting mutations in the first attenuator region of the *Bacillus subtilis pyr* operon that are defective in pyrimidine-mediated regulation of expression. J. Bacteriol. **178:** 2351–2355.
15. **Ghim, S.-Y., and J. Neuhard.** 1994. The pyrimidine biosynthesis operon of the thermophile *Bacillus caldolyticus* includes genes for uracil phosphoribosyl transferase and uracil permease. J. Bacteriol. **176:**3698–3707.
16. **Ghim, S.-Y., P. Nielsen, and J. Neuhard.** 1994. Molecular characterization of pyrimidine biosynthesis genes from the thermophile *Bacillus caldolyticus*. Microbiology **140:**479–491.
17. **Glansdorff, N.** 1965. Topography of cotransducible arginine mutations in *Escherichia coli* K-12. Genetics **51:**167–179.
18. **Grogan, D. W., and R. P. Gunsalus.** 1993. *Sulfolobus acidocaldarius* synthesizes UMP via a standard de novo pathway: results of a biochemical-genetic study. J. Bacteriol. **175:**1500–1507.
19. **Hartmann, R. K., and V. A. Erdmann.** 1989. *Thermus thermophilus* 16S rRNA is transcribed from an isolated transcriptional unit. J. Bacteriol. **171:** 2933–2941.
20. **Hawley, D. K., and W. R. McClure.** 1983. Compilation and analysis of *Escherichia coli* promoter DNA sequences. Nucleic Acids Res. **11:**2237–2255.
21. **Honzatko, R. B., J. L. Crawford, H. L. Monaco, J. E. Ladner, B. F. P. Edwards, D. R. Evans, S. G. Warren, D. C. Wiley, R. C. Ladner, and W. N. Lipscomb.** 1982. Crystal and molecular structures of native and CTP-liganded aspartate carbamoyltransferase. J. Mol. Biol. **160:**219–263.
22. **Imada, K., M. Sato, N. Tanaka, Y. Katsube, Y. Matsumura, and T. Oshima.** 1991. Three-dimensional structure of highly thermostable enzyme, 3-isopropylmalate dehydrogenase of *Thermus thermophilus* at 2.2 A resolution. J. Mol. Biol. **222:**725–738.
23. **Kelly, C. A., M. Nishiyama, Y. Ohnishi, T. Beppu, and J. Birktoft.** 1993. Determinants of protein thermostability observed in the 1.9-A crystal structure of malate dehydrogenase from the thermophilic bacterium *Thermus flavus*. Biochemistry **32:**3913–3922.
24. **Kenny, M. J., D. McPhail, and M. Shepherdson.** 1996. A reappraisal of the diversity and class distribution of aspartate transcarbamoylases in Gram-negative bacteria. Microbiology **142:**1873–1879.
25. **Kreutzer, R., V. Kruft, E. V. Bobkova, O. I. Lavrik, and M. Sprinzl.** 1992. Structure of the phenylalanyl-tRNA synthetase genes from *Thermus thermophilus* HB8 and their expression in *Escherichia coli*. Nucleic Acids Res. **20:**4173–4178.
26. **Kumar, A. P., D. M. Brichta, M. J. Schurr, and G. A. O'Donovan.** 1994. Deletion of a 34 amino acid N-terminal region of the aspartate transcarbamoylase in *Pseudomonas putida* abolishes regulatory nucleotide effector responses, abstr. K-36, p. 282. *In* Abstracts of the 94th General Meeting of the American Society for Microbiology 1994. American Society for Microbiology, Washington, D.C.
27. **Legrain, C., M. Demarez, N. Glansdorff, and A. Piérard.** 1995. Ammonia-dependent synthesis and metabolic channelling of carbamoylphosphate in the hyperthermophilic archaeon *Pyrococcus furiosus*. Microbiology **141:**1093–1099.
28. **Lipscomb, W. N.** 1994. Aspartate transcarbamoylase from *Escherichia coli*; activity and regulation. Adv. Enzymol. **68:**67–152.
29. **Lu, Y., R. J. Turner, and R. L. Switzer.** 1995. Roles of three transcriptional attenuators of the *Bacillus subtilis* pyrimidine biosynthetic operon in the regulation of its expression. J. Bacteriol. **177:**1315–1325.
30. **Lu, Y., and R. L. Switzer.** 1996. Evidence that the *Bacillus subtilis* pyrimidine regulatory protein PyrR acts by binding to *pyr* mRNA at three sites in vivo. J. Bacteriol. **178:**5806–5809.
31. **Martinussen, J., P. Glaser, P. S. Andersen, and H. H. Saxild.** 1995. Two genes encoding uracil phosphoribosyltransferase are present in *Bacillus subtilis*. J. Bacteriol. **177:**271–274.
32. **Menendez-Arias, L., and P. Argos.** 1989. Engineering protein thermal stability. Sequence statistics point to residue substitutions in alpha helices. J. Mol. Biol. **206:**397–406.
33. **Miyazaki, K., H. Eguchi, A. Yamagishi, T. Wakagi, and T. Oshima.** 1992. Molecular cloning of the isocitrate dehydrogenase gene of an extreme thermophile, *Thermus thermophilus* HB8. Appl. Environ. Microbiol. **58:**93–98.
34. **Mrabet, N. T., A. Van de Broeck, I. Van den Brande, P. Stanssens, Y. Laroche, A. M. Lambeir, G. Matthijsens, J. Jenkins, M. Chiadmi, H. Van Tilbeurgh, F. Rey, J. Janin, W. J. Quax, I. Lasters, M. D. Mayer, and S. J. Wodak.** 1992. Arginine residues as stabilizing elements in proteins. Biochemistry **31:**2239–2253.
35. **Oshima, T., and K. Imahori.** 1974. Description of *Thermus thermophilus* comb. nov., a non-sporulating thermophilic bacterium from a Japanese thermal spa. Int. J. Syst. Bacteriol. **24:**102–112.
36. **Piérard, A., and J. M. Wiame.** 1964. Regulation and mutation affecting a glutamine dependent formation of carbamyl phosphate in *Escherichia coli*. Biochem. Biophys. Res. Commun. **15:**76.
37. **Prescott, L. M., and M. E. Jones.** 1969. Modified methods for the determination of carbamyl aspartate. Anal. Biochem. **32:**408–419.
38. **Purcarea, C., G. Erauson, D. Prieur, and G. Hervé.** 1994. The catalytic and regulatory properties of aspartate transcarbamoylase from *Pyrococcus abyssi*, a new deep-sea hyperthermophilic archeobacterium. Microbiology **140:**1967–1975.
39. **Quinn, C. L., B. T. Stephenson, and R. L. Switzer.** 1991. Functional organization and nucleotide sequence of the *Bacillus subtilis* pyrimidine biosynthetic operon. J. Biol. Chem. **266:**9113–9127.
40. **Rentier-Delrue, F., S. C. Manole, S. Moyens, P. Terpstra, V. Mainfroid, K. Goraj, M. Lion, W. Hol, and J. A. Martial.** 1993. Cloning and overexpression of the triosephosphate isomerase genes from psychrophilic and thermophilic bacteria. Structural comparison of the predicted protein sequences. J. Mol. Biol. **229:**85–93.
41. **Roland, K. L., F. E. Powell, and C. L. Turnbough, Jr.** 1985. Role of translation and attenuation in the control of *pyrBI* operon expression in *Escherichia coli* K-12. J. Bacteriol. **163:**991–999.
42. **Roof, W. D., K. F. Foltermann, and J. R. Wild.** 1982. The organization and regulation of the *pyrBI* operon in *E. coli* includes a rho-independent attenuator sequence. Mol. Gen. Genet. **187:**391–400.
43. **Rosenberg, M., and D. Court.** 1979. Regulatory sequences involved in the promotion and termination of RNA transcription. Annu. Rev. Genet. **13:** 319–353.
44. **Sambrook, J., E. F. Fritsch, and T. Maniatis.** 1989. Molecular cloning: a laboratory manual. Cold Spring Harbor Laboratory, Cold Spring Harbor, N.Y.
45. **Sanger, F., S. Nicklen, and A. R. Coulson.** 1977. DNA sequencing with chain-terminating inhibitors. Proc. Natl. Acad. Sci. USA **74:**5463–5467.
46. **Sato, S., Y. Nakada, S. Kanaya, and T. Tanaka.** 1988. Molecular cloning and nucleotide sequence of *Thermus thermophilus* HB8 *trpE* and *trpG*. Biochim. Biophys. Acta **950:**303–312.
47. **Schurr, M. J., J. F. Vickrey, A. P. Kumar, A. L. Campbell, R. Cunin, R. C. Benjamin, M. S. Shanley, and G. A. O'Donovan.** 1995. Aspartate transcarbamoylase genes of *Pseudomonas putida*: requirement for an inactive dihydroorotase for assembly into the dodecameric holoenzyme. J. Bacteriol. **177:**1751–1759.
48. **Shaw, W. V.** 1975. Chloramphenicol acetyltransferase from chloramphenicol-resistant bacteria. Methods Enzymol. **43:**737–755.
48a. **Shepherdson, M.** Personal communication.
49. **Shepherdson, M., and D. Mc Phail.** 1993. Purification of aspartate transcarbamoylase from *Pseudomonas syringae*. FEMS Microbiol. Lett. **114:**201–206.
50. **Short, J. M., J. M. Fernandez, J. A. Sorge, and W. D. Huse.** 1988. λZAP: a bacteriophage λ expression vector with in vivo excission properties. Nucleic Acids Res. **16:**7583–7600.

51. **Simmer, J. P., R. E. Kelly, A. G. Rinker, Jr., B. H. Zimmermann, J. L. Scully, H. Kim, and D. R. Evans.** 1990. Mammalian dihydroorotase: nucleotide sequence, peptide sequences, and evolution of the dihydroorotase domain of the multifunctional protein CAD. Proc. Natl. Acad. Sci. USA **87:**174–178.
52. **Stevens, R. C., K. M. Reinisch, and W. N. Lipscomb.** 1991. Molecular structure of *Bacillus subtilis* aspartate transcarbamoylase at 3.0 A resolution. Proc. Natl. Acad. Sci. USA **88:**6087–6091.
53. **Tinoco, I., P. N. Borer, B. Dengler, M. D. Levine, O. C. Uhlenbeck, D. M. Crothers, and J. Gralla.** 1973. Improved estimation of secondary structure in ribonucleic acids. Nature New Biol. **246:**40–41.
54. **Turnbough, C. L., Jr., K. L. Hicks, and J. P. Donahue.** 1983. Attenuation control of *pyrBI* operon expression in *Escherichia coli* K12. Proc. Natl. Acad. Sci. USA **80:**368–372.
55. **Turner, R. J., Y. Lu, and R. L. Switzer.** 1994. Regulation of the *Bacillus subtilis* pyrimidine biosynthetic (*pyr*) gene cluster by an autogenous transcriptional attenuation mechanism. J. Bacteriol. **176:**3708–3722.
56. **Van de Casteele, M., and P. G. Chen.** Unpublished data.
57. **Van de Casteele, M., M. Demarez, C. Legrain, and N. Glansdorff.** 1990. Pathways of arginine biosynthesis in extreme thermophilic archeo- and eubacteria. J. Gen. Microbiol. **136:**1177–1183.
58. **Van de Casteele, M., L. Desmarez, C. Legrain, P. G. Chen, K. Van Lierde, A. Piérard, and N. Glansdorff.** 1994. Genes encoding aspartate carbamoyltransferase of *Thermus aquaticus* ZO5 and *Thermotoga maritima* MSB8: modes of expression in *E. coli* and properties of their products. Biocatalysis **112:**165–179.
59. **Van de Casteele, M., C. Legrain, L. Desmarez, P. G. Chen, A. Piérard, and N. Glansdorff.** Molecular physiology of carbamoylation under extreme conditions: what can we learn from extreme thermophilic microorganisms? Comp. Biochem. Physiology, in press.
60. **Vieira, J., and J. Messing.** 1982. The pUC plasmids, an M13mp7-derived system for insertion mutagenesis and sequencing with synthetic universal primers. Gene **19:**259–268.
61. **Vonstein, V., S. P. Johnson, H. Yu, M. J. Casadaban, N. C. Pagratis, J. M. Weber, and D. Demirjian.** 1995. Molecular cloning of the *pyrE* gene from the extreme thermophile *Thermus flavus*. J. Bacteriol. **177:**4540–4543.
62. **Watanabe, K., K. Chishiro, K. Kitamura, and Y. Suzuki.** 1991. Proline residues responsible for thermostability occur with high frequency in the loop regions of an extremely thermostable oligo-1,6-glucosidase from *Bacillus thermoglucosidasius* KP1006. J. Biol. Chem. **266:**24287–24294.
63. **Woese, C. R.** 1987. Bacterial evolution. Microbiol. Rev. **51:**221–271.
64. **Yamagishi, A., T. Tanimoto, T. Suzuki, and T. Oshima.** 1996. Pyrimidine biosynthesis genes (*pyrE* and *pyrF*) of an extreme thermophile, *Thermus thermophilus*. Appl. Environ. Microbiol. **62:**2191–2194.
65. **Zuker, M., and P. Stiegler.** 1981. Optimal computer folding of large RNA sequences using thermodynamics and auxiliary information. Nucleic Acids Res. **9:**133–148.